

Self-Sorting of Polyelectrolyte–Amphiphile Complexes on a Graphite Surface

N. Severin,[†] I. M. Sokolov,^{*,†} N. Miyashita,[‡] D. G. Kurth,^{*,§} and J. P. Rabe[†]

Department of Physics, Humboldt University Berlin, Newtonstr. 15, D-12489 Berlin, Germany;
Max-Planck Institute of Colloids and Interfaces, Research Campus Golm, D-14424 Potsdam, Germany;
and National Institute for Materials Science, Tsukuba, Japan

Received May 2, 2007

ABSTRACT: We investigate the self-assembly of polydisperse polyelectrolyte–amphiphile complexes (PACs) on the basal plane of highly ordered pyrolytic graphite (HOPG) at submonolayer coverage. The PACs assemble as straight rods that organize into raftlike structures on the surface. We find length self-sorting of PACs in the rafts such that each PAC neighbors preferably a PAC of similar length on each side. We show that the observed length segregation can be explained by pairwise interactions.

Introduction

Self-assembly of molecules on surfaces and interfaces is an attractive way to study the assembly processes at the nanometer scale¹ since scanning probe microscopies exhibit higher resolution than bulk microscopies. On the other hand, interaction forces with the surface may affect the assembly.^{2,3} At surfaces and interfaces, self-assembly mechanisms associated with hydrogen bonding,^{2,4–6} dipolar coupling,⁷ or metal coordination^{8,9} have been studied. Here, we discuss the self-organization of weakly interacting polyelectrolyte–amphiphile complexes (PACs) into raftlike structures on basal plane of graphite and provide new experimental results and theoretical insights for the organization of supramolecular structures on surfaces.

The PAC used here consists of a poly(styrenesulfonate) backbone decorated with ionic amphiphiles, which are attached to the backbone through electrostatic interactions of ammonium head groups and the oppositely charged sulfonate groups. PACs assemble into raftlike structures of highly oriented and fully extended PACs on a graphite surface, when spin-coated from chloroform solution.¹⁰ The stretching of PACs is attributed to the interaction of the alkyl tails of the amphiphiles with the substrate. The formation of the raftlike structures is related to the initial mobility of PACs on the surface. As we will show in this paper, the self-assembly of rafts is accompanied by length segregation of PACs, such that PACs of similar length tend to be neighbors in the structure. Overall, raft formation, therefore, corresponds to a self-sorting process. We provide a theoretical description of this effect, which also gives us an estimate of the interaction energy of PACs on the surface per unit length.

Materials and Methods

PACs were prepared from poly(sodium 4-styrenesulfonate) (PSS) and trimethylhexadecylammonium bromide (THA Br) as described before,¹¹ except that water was used for washing the PACs. PSS was purchased from Aldrich: $M_n = 72.820$, $M_w = 98.870$, $D = 1.36$ (sample A in ref 10). We have chosen a sample with the relatively broad chain length distribution, since it is especially suitable for length segregation analysis. A chloroform solution of PACs at concentration of 10^{-2} mg/mL was spin-coated onto a

freshly cleaved graphite surface (ZYH grade) at 40 rounds per second (rps). The samples were imaged with scanning force microscopy (SFM) either right after solution application to demonstrate the dynamics of PACs aggregation or after annealing for 15 min at 35 °C for length segregation analysis. SFM imaging was performed with a multimode scanning probe microscope (Digital Instruments Inc., Santa Barbara, CA) operating in tapping mode at ambient conditions with etched silicon cantilevers (Olympus) with a typical resonance frequency of 70 kHz and a spring constant of 2 N/m. The length analysis was performed with a home-built software package. We characterized the length segregation of PACs by the difference in length between neighboring PACs, which we will call δ .

Experimental Results

Imaging the samples at room temperature shortly after spin-coating reveals disordered, fuzzy patterns on the graphite surface. The shape of the patterns changes from scan to scan (Figure 1a). After 5–10 min, periodic structures begin to appear, which still undergo shape changes (Figure 1b,c). Roughly half an hour after spin-coating, stable raftlike structures of tightly packed PAC rods are observed (Figure 1d).¹⁰ However, the shape of the final structures under these conditions is not representative because the SFM tip influences the formation of aggregates and also the surface temperature is not controlled. For the analysis of the length distribution, the samples were imaged after annealing for 15 min at 35 °C.

The length of the rods is directly determined from SFM images (Figure 2). Only those PACs are taken into account, which could be clearly resolved from one end to another; no additional sorting has been performed. In order to compare the data with the length distribution of the parent PSS, we apply a correction for the length due to the tip convolution effect. The lengthening is estimated in the following way. The apparent width of isolated PACs is 6–8 nm and the height is 0.7–1 nm, which are in a good agreement with the apparent size of isolated PSS molecules imaged with the same tips.¹² Since the diameter of a PSS molecule is roughly 1 nm, we estimate the broadening due to the tip convolution effect to be 6 ± 1 nm. For the length correction, 6 nm is subtracted from the experimentally determined PAC length. The correction is relatively small compared to the average PAC length. Moreover, while the length correction affects the calculation of length distribution, it does not affect the lengths difference, δ , which is of primary interest in what follows.

* Corresponding author. E-mail: igor.sokolov@physik.hu-berlin.de.

[†] Humboldt University Berlin.

[‡] Max-Planck Institute of Colloids and Interfaces.

[§] National Institute for Materials Science.

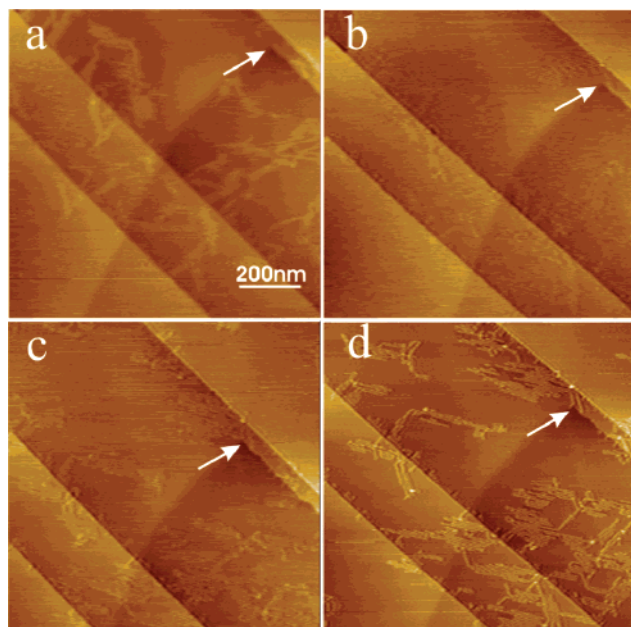


Figure 1. SFM images of the same area taken at different times after spin-coating of PAC from chloroform solution onto a graphite surface. The arrows indicate the same graphite surface defect on all four images and are a guide for eye. The images are taken approximately (a) 5, (b) 10, (c) 17, and (d) 45 min after spin-coating.

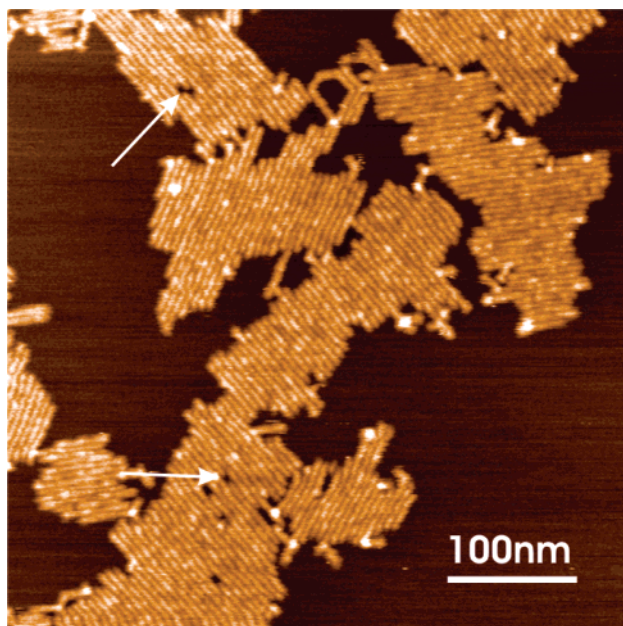


Figure 2. Raftlike PAC structures on graphite. The rods are considered to be single PACs. Most PACs neighbor exactly one PAC on each side: only in a few cases, a longer PAC neighbors several shorter PACs as indicated by the arrows. PACs follow the hexagonal symmetry (60° rotational symmetry) of the graphite substrate.

In order to compare the PAC length distribution from the image analysis with the distribution of the parent PSS, we recalculated the length distribution into a mass distribution assuming the projected length of the PAC repeat unit to be 0.216 nm^{10} and the molar mass of the PSS repeat unit to be 206 g/mol . The number-average and weight-average of the molecular weights are $M_n = 71\,300$ and $M_w = 91\,000$, respectively, so that $D \equiv M_w/M_n = 1.28$. The mass distribution determined from SFM analysis is somewhat narrower than the distribution of the parent PSS ($D = 1.36$). This is not surprising: First, it is difficult to determine the length of objects that are shorter than roughly 20 nm due to the limited SFM resolution; therefore,

short objects were mostly not counted. Second, long PACs that extend beyond the image are not counted because they are not completely visible. Taking these arguments into account, we propose that the length distribution of the PACs on the surface is comparable to the native PSS. We assume, therefore, that the imaged rods consist of single PACs and not of an assembly of short pieces, which corroborates with previous findings.¹⁰

Generally, neighboring PACs consist of one polymer each. Only in a few cases (less than 5%) two or more short rods assemble along a long PAC (Figure 2). A comparison of experimentally determined length difference distributions of neighboring PACs $p(\delta)$ and random pairs of polymers $p_{\text{rand}}(\delta)$ reveals a significant length segregation (Figure 3a).

Theory

We assume that the PACs remain mobile long enough for the system to equilibrate and retain the acquired structure under solvent evaporation. The equilibrium structure is defined by the tradeoff between lowering the potential energy due to contact between the rods and the corresponding loss in translational entropy (canonical ensemble under temperature T). Assuming the interaction between the rods to be short-range, we can consider the raft to consist of independent pairs of rods in contact and the rods from different rafts not to interact with each other. The overall energy of the system is the sum of the energies of interaction of pairs of neighboring rods. Now we concentrate on one raft and discuss the rods' ordering with respect to their length.

We characterize pairs by the distance Δx between the ends and their length difference δ . To estimate the distribution of the neighbor's lengths differences, let us consider a one-dimensional cluster of parallel rods, which are free to translate along their axes. Let us assume that rod 1 is longer than rod 2, $L_1 > L_2$. If the end of rod 1 is situated at zero and the position of the end of the adjacent rod 2 is at x , then the length of the portion at contact of the two rods has a trapezoidal dependence on x :

$$l(x, L_1, L_2) = \begin{cases} 0, & x < -L_2 \\ L_2 - x, & -L_2 < x < 0 \\ L_2, & 0 < x < L_1 - L_2 \\ L_1 - x, & L_1 - L_2 < x < L_1 \\ 0, & x > L_1 \end{cases}$$

The situations with $x < -L_2$ and $x > L_1$ are not considered as cases when the pair of molecules belongs to the same domain, i.e., are not counted as parts of our statistical ensemble. Without further assumption, which molecule in a pair of molecules of length L_1 and L_2 is longer, we get the length of the shorter molecule as $l_2 \equiv \frac{1}{2}(L_1 + L_2 - |L_1 - L_2|)$ and the length of the longer one as $l_1 \equiv \frac{1}{2}(L_1 + L_2 + |L_1 - L_2|)$, which defines the overlap length $l(x, L_1, L_2)$. The lengths of counted PACs are much longer than the length of one PSS repeat unit; therefore, it is reasonable to simplify PACs as homogeneous rods with interaction energy per unit length of contact u . We assume here and rationalize later that the immobilization of PACs is caused by the stepwise variation of the interaction energy density u . The interaction energy $E(x, L_1, L_2)$ of two molecules of L_1 and L_2 lengths is thus $ul(x, L_1, L_2)$. The overall energy of $N - 1$ pairs of N molecules forming the cluster is $H = u \sum_{i=1}^{N-1} l(x_i, L_i, L_{i+1})$, which defines the Boltzmann factor for the corresponding configuration $w = \exp(-H/k_B T)$. Since we are only interested in the weight of different arrangements (i.e., the dependence of

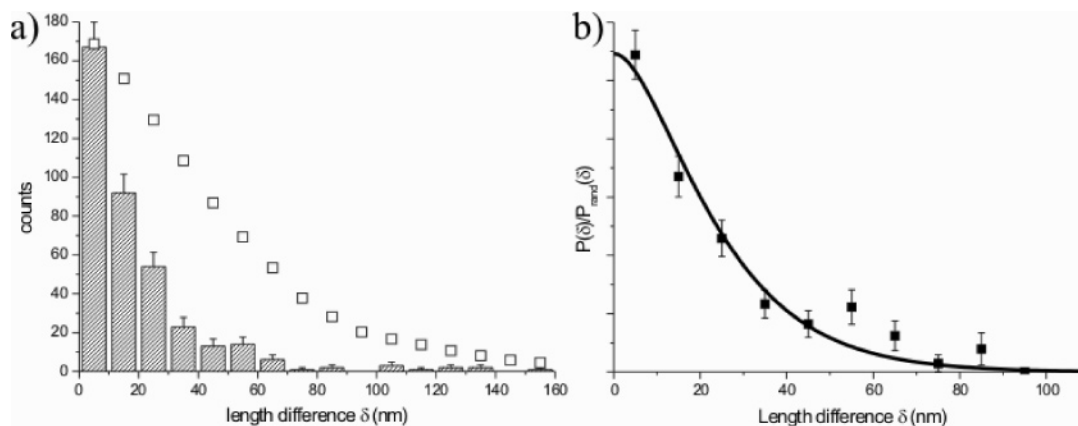


Figure 3. (a) Histogram: the length difference between neighboring molecules in raftlike structures ($\sim p(\delta)$). Open squares: the scaled length difference of all possible combinations of molecules involved in counting of the histogram corresponding to a random length distribution ($\sim p_{\text{rand}}(\delta)$). (b) $p(\delta)/p_{\text{rand}}(\delta)$ (squares) and fit with eq 1 (solid line). The abscissa is limited to 100 nm, since a length difference of more than 100 nm does not contribute substantially to the fit due to low counts and correspondingly high errors.

w on L_i), we integrate the weights over all possible values of x_i . The corresponding values of x_i are those for which the overlap between the neighboring molecules exists; otherwise, they are not considered as belonging to one cluster. The configuration integral over the translational degrees of freedom of the molecules belonging to the same cluster $\int dx_1 \dots dx_{N-1} \exp(-H/kT)$ thus reads

$$\int dx_1 \dots dx_{N-1} \exp\left(-\frac{H}{k_B T}\right) = \prod_{i=1}^{N-1} \int dx_i \exp\left(-\frac{u}{k_B T} l(x_i, L_i, L_{i+1})\right)$$

In the case of self-assembly, the value of $\epsilon = -u/k_B T$ is positive (attraction). The overall argument of the exponential $\epsilon l(x, L_1, L_2)$ for a typical pair of molecules belonging to the same cluster is, therefore, positive and large. A single integral over x is rather trivial:

$$\begin{aligned} \int_{-L_2}^{L_1} \exp(-\epsilon l(x, L_1, L_2)) dx &= \frac{2}{\epsilon} (\exp(-L_2) - 1) + \\ &\quad (L_1 - L_2) \exp(\epsilon L_2) \\ &= -\frac{2}{\epsilon} + \left(|L_1 - L_2| + \frac{2}{\epsilon} \right) \exp\left(\frac{\epsilon}{2}(L_1 + L_2) - |L_1 - L_2|\right) \end{aligned}$$

Since the argument of the exponential is considered to be large, the first term can be neglected and we have

$$\begin{aligned} \int_{-L_2}^{L_1} \exp(-\epsilon l(x, L_1, L_2)) dx &\approx \left(|L_1 - L_2| + \frac{2}{\epsilon} \right) \times \\ &\quad \exp\left(\frac{\epsilon}{2}(L_1 + L_2) - |L_1 - L_2|\right) \\ &= \exp\left[\frac{\epsilon}{2}(L_1 + L_2) - \frac{2}{\epsilon} |L_1 - L_2| + \ln\left(|L_1 - L_2| + \frac{2}{\epsilon}\right)\right] \end{aligned}$$

The overall configuration integral is then

$$\begin{aligned} \int dx_1 \dots dx_{N-1} \exp\left(-\frac{H}{k_B T}\right) &= \\ &\exp\left(\frac{\epsilon}{2} \sum_{i=1}^N (L_i + L_{i+1})\right) \exp\left[\sum_{i=1}^{N-1} \left(-\frac{2}{\epsilon} \delta_i + \ln\left(\delta_i + \frac{2}{\epsilon}\right)\right)\right] \end{aligned}$$

where $\delta = |L_i - L_{i+1}|$. The first term for a large cluster tends to be $\exp(\epsilon N \langle l \rangle)$, where $\langle l \rangle$ is the mean length of the molecule and does not depend on the arrangement of the molecules in a cluster (up to finite size effects caused by the first and the last

term in the sum). Thus, the Boltzmann weight for finding a pair of neighboring molecules which differ in their length by a value of δ is

$$w(\delta) = \left(\delta + \frac{2}{\epsilon}\right) \exp\left[-\frac{2}{\epsilon} \delta\right]$$

From this the probability density function of the difference of the molecule length can be obtained by the change of variables to $\delta = L_i - L_{i+1}$ and $y = (L_i + L_{i+1})/2$ with $L_1 = y + \delta/2$ and $L_2 = y - \delta/2$. The Jacobian of this transformation is -1 and therefore

$$p(\delta, y) \propto p(y + \delta/2) p(y - \delta/2) \left[\left(\delta + \frac{2}{\epsilon}\right) \exp(-\epsilon |\delta|/2) \right]$$

The marginal distribution in the length's difference is given by integration over y . Note that $p_{\text{rand}}(\delta) = 2 \int_{\delta/2}^{\infty} p(y + \delta/2) p(y - \delta/2) dy$ gives us the distribution of differences in the molecule's lengths in a randomized array of molecules, and therefore

$$p(\delta) = N(\epsilon) p_{\text{rand}}(\delta) \left[\left(\delta + \frac{2}{\epsilon}\right) \exp(-\epsilon |\delta|/2) \right] \quad (1)$$

where $N(\epsilon)$ is the normalization constant:

$$N(\epsilon) = \left\{ \int_{\delta/2}^{\infty} p_{\text{rand}}(\delta) \left[\left(\delta + \frac{2}{\epsilon}\right) \exp(-\epsilon |\delta|/2) d\delta \right]^{-1} \right\}^{-1}$$

This expression holds already for moderate $\epsilon \delta$ of the order of $k_B T$.

Discussion

Importantly, eq 1 has only one fitting parameter, ϵ . Fitting the experimental normalized length difference distribution $p(\delta)/p_{\text{rand}}(\delta)$ to eq 1 yields $\epsilon = 0.15 \pm 0.01 k_B T/\text{nm}$ (Figure 3b) or $0.03 k_B T$ per repeat unit of PAC. This is a rather weak interaction energy compared to for instance hydrogen bonds. However, the interaction energy of two PACs of 80 nm length, which is the average length of PACs, totals $12 k_B T$, being high enough to cause strong length ordering. Interaction energies for two average length PACs ($12 k_B T$) match the enthalpy of evaporation of volatile liquids molecules which evaporate relatively fast on a time scale of minutes. This is also the characteristic time scale

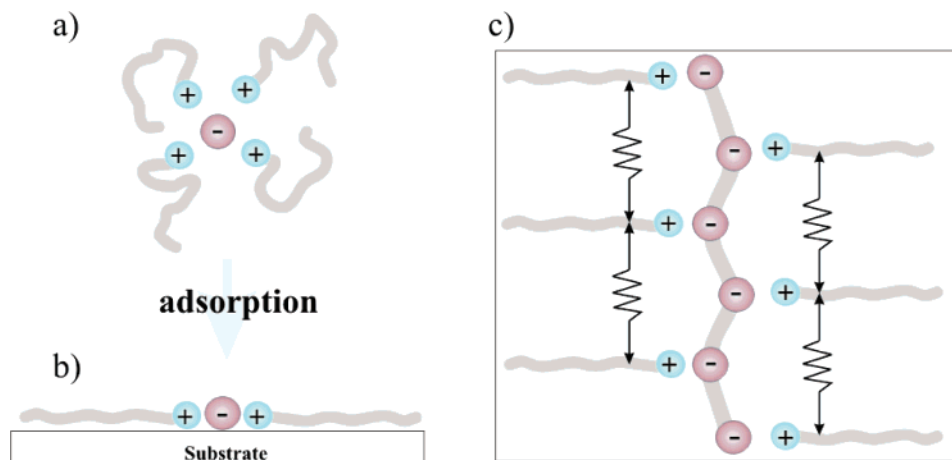


Figure 4. In organic solvents the amphiphiles encapsulate the hydrophilic PSS backbone¹⁹ (side view a). Adsorption of PAC on graphite forces the alkyl chains along the lattice axis in order to maximize the adsorption energy (side view b). Self-assembly of the alkyl chains along the lattice axis stretches the PSS backbone. The projected length of two repeat units in the preferred anti conformation (0.43 nm) is comparable to or even smaller than a typical distance between amphiphile molecules in a crystalline monolayer on graphite (0.45 nm for octadecylamine, for example, as can be estimated from ref 20) (top view c).

of the possible rods' rearrangements. This fact confirms our theoretical assumption of the equilibration of the system during the raft formation.

So far there is no experimental evidence that PAC aggregates in solution at this concentration. It is therefore reasonable to assume that self-organization of PAC rafts occurs on the surface. For highly volatile solvents spin-coating can be modeled as drying of a thin uniform liquid film, which leaves a uniform layer of solute on the surface.¹³ The amount of PAC deposited on the surface can be directly estimated from SFM images. Here we determine the molecular number surface density (number of molecules divided by the inspected area) multiplied by the mean weight of the molecule: $\sim 10^{-4}$ g/m² of PAC is deposited on the surface. At the given concentration this corresponds to an initial film thickness of liquid of 10 μ m. Taking into account an apparent height of a PAC rod of 1 nm, the concentration increases during spin-coating by roughly 4 orders of magnitude. The drastic increase of the concentration drives the self-organization of PACs into well-ordered domains.

The straightening of PACs on the surface can be rationalized by considering the interactions of the amphiphiles with graphite.¹⁰ If a PAC adsorbs as straight rod, all alkyl chains can adsorb on the underlying substrate, thus maximizing the adsorption energy.¹⁴ The spacing of amphiphile molecules in a crystalline monolayer on graphite is close to the projected length of two PSS repeat units in the preferred anti conformation (Figure 4). Assembly of the amphiphiles along the lattice axis in two parallel, head-to-head oriented, staggered rows, therefore, causes efficient stretching of the PSS backbone. In fact, the PAC on the surface may be regarded as an overstretched helix. The straightening facilitates organization of PACs into rafts because it eliminates the conformational entropy cost that works against ordering.

The equilibration of the system on the surface requires mobility of PACs across the surface as well as assembly and disassembly of aggregates; on the other hand, the clear SFM images of the final structures require their immobilization on the surface. While a volatile liquid evaporates macroscopically relatively fast after spin-coating, an ultrathin liquid film remains on the surface for a longer time.¹⁵ Ultrathin liquid films on solid surfaces differ from the bulk liquid state since they order in molecular layers parallel to the substrate surface.¹⁶ Evaporation of the ultrathin liquid films is not linear but occurs layerwise

and stepwise in time.¹⁷ During this time the PACs remain mobile. The stepwise evaporation of the liquid film supports the assumption of the stepwise variation of the interaction energy density ϵ and correspondingly the fast transition between the mobile state and the full immobilization of PACs which fixes the structures formed during the mobility stage and allows for their SFM observation. The estimated interaction energy density ϵ is thus the energy difference between PAC neighboring another PACs and isolated PAC enclosed by solvent molecules. The difference in interaction energies is reasonably small in comparison with, for example, the interaction energy of two straight alkyl chains oriented parallel to each other: $1.7 k_B T/\text{nm}$ (as can be estimated from ref 18). Drying of the solvent layer increases the value of ϵ by an order of magnitude, causing freezing of the raftlike structures.

Conclusions and Outlook

We have investigated the self-assembly of polyelectrolyte–amphiphile complexes (PACs) in raftlike structures on the basal plane surface of graphite and demonstrated that the simple model of rods with pairwise interactions, characterized by the interaction energy per unit length, explains the observed length segregation of the PACs. Although we restricted our investigation to low surface coverage of PACs (leading to a simple theoretical description within the model discussed above), experiments with higher surface coverage up to a monolayer coverage can be envisioned to aid in further understanding of length segregation in liquid crystalline polymers.²¹ In this case the geometric restrictions can hinder the mobility of the molecules and lead to the appearance of metastable structures. Experiments with longer PACs can serve as a model system for processes in polymer systems. Self-assembly of self-assembling polymers⁸ on surfaces will provide an interesting opportunity to control the size of the aggregates, for instance, for the fabrication of well-defined nanoarchitectures by self-assembly.

Acknowledgment. The authors thank Jörg Barner (Humboldt University Berlin) for providing image analysis software. Support from SFB 448 is gratefully acknowledged.

References and Notes

- (1) Cerda, J.; Michaelides, A.; Bocquet, M. L.; Feibelman, P. J.; Mitsui, T.; Rose, M.; Fomin, E.; Salmeron, M. Novel water overlayer growth

- on Pd(111) characterized with scanning tunneling microscopy and density functional theory. *Phys. Rev. Lett.* **2004**, *93*, 116101.
- (2) Rabe, J. P.; Buchholz, S. Commensurability and Mobility in 2-Dimensional Molecular-Patterns on Graphite. *Science* **1991**, *253*, 424–427.
 - (3) Samori, P.; Severin, N.; Mullen, K.; Rabe, J. P. Macromolecular fractionation of rod-like polymers at atomically flat solid-liquid interfaces. *Adv. Mater.* **2000**, *12*, 579–582.
 - (4) Buchholz, S.; Rabe, J. P. Molecular Imaging of Alkanol Monolayers on Graphite. *Angew. Chem., Int. Ed. Engl.* **1992**, *31*, 189–191.
 - (5) Barth, J. V.; Weckesser, J.; Cai, C. Z.; Gunter, P.; Burgi, L.; Jeandupeux, O.; Kern, K. Building supramolecular nanostructures at surfaces by hydrogen bonding. *Angew. Chem., Int. Ed.* **2000**, *39*, 1230–1234.
 - (6) Keeling, D. L.; Oxtoby, N. S.; Wilson, C.; Humphry, M. J.; Champness, N. R.; Beton, P. H. Assembly and processing of hydrogen bond induced supramolecular nanostructures. *Nano Lett.* **2003**, *3*, 9–12.
 - (7) Yokoyama, T.; Yokoyama, S.; Kamikado, T.; Okuno, Y.; Mashiko, S. Selective assembly on a surface of supramolecular aggregates with controlled size and shape. *Nature (London)* **2001**, *413*, 619–621.
 - (8) Kurth, D. G.; Severin, N.; Rabe, J. P. Perfectly straight nanostructures of metallosupramolecular coordination-polyelectrolyte amphiphile complexes on graphite. *Angew. Chem., Int. Ed.* **2002**, *41*, 3681–3683.
 - (9) Lin, N.; Dmitriev, A.; Weckesser, J.; Barth, J. V.; Kern, K. Real-time single-molecule imaging of the formation and dynamics of coordination compounds. *Angew. Chem., Int. Ed.* **2002**, *41*, 4779–4783.
 - (10) Severin, N.; Rabe, J. P.; Kurth, D. G. Fully extended polyelectrolyte-amphiphile complexes adsorbed on graphite. *J. Am. Chem. Soc.* **2004**, *126*, 3696–3697.
 - (11) Antonietti, M.; Conrad, J.; Thunemann, A. Polyelectrolyte-Surfactant Complexes—A New Type of Solid, Mesomorphous Material. *Macromolecules* **1994**, *27*, 6007–6011.
 - (12) Severin, N.; Okhapkin, I. M.; Khokhlov, A. R.; Rabe, J. P. Adsorption of polyelectrolyte molecules to a nanostructured monolayer of amphiphiles. *Nano Lett.* **2006**, *6*, 1018–1022.
 - (13) Emslie, A. G.; Bonner, F. T.; Peck, L. G. Flow of a Viscous Liquid on a Rotating Disk. *J. Appl. Phys.* **1958**, *29*, 858–862.
 - (14) Sheiko, S. S.; Sun, F. C.; Randall, A.; Shirvanyants, D.; Rubinstein, M.; Lee, H.; Matyjaszewski, K. Adsorption-induced scission of carbon-carbon bonds. *Nature (London)* **2006**, *440*, 191–194.
 - (15) Severin, N.; Zhuang, W.; Ecker, C.; Kalachev, A. A.; Sokolov, I. M.; Rabe, J. P. Blowing DNA bubbles. *Nano Lett.* **2006**, *6*, 2561–2566.
 - (16) Horn, R. G.; Israelachvili, J. N. Direct Measurement of Structural Forces Between 2 Surfaces in a Non-Polar Liquid. *J. Chem. Phys.* **1981**, *75*, 1400–1411.
 - (17) Forcada, M. L.; Mate, C. M. Molecular Layering During Evaporation of Ultrathin Liquid-Films. *Nature (London)* **1993**, *363*, 527–529.
 - (18) Hentschke, R.; Schurmann, B. L.; Rabe, J. P. Molecular-Dynamics Simulations of Ordered Alkane Chains Physisorbed on Graphite. *J. Chem. Phys.* **1992**, *96*, 6213–6221.
 - (19) von Ferber, C.; Lowen, H. Complexes of polyelectrolytes and oppositely charged ionic surfactants. *J. Chem. Phys.* **2003**, *118*, 10774–10779.
 - (20) Cyr, D. M.; Venkataraman, B.; Flynn, G. W.; Black, A.; Whitesides, G. M. Functional group identification in scanning tunneling microscopy of molecular adsorbates. *J. Phys. Chem.* **1996**, *100*, 13747–13759.
 - (21) Wang, W.; Lieser, G.; Wegner, G. Extended-Chain Lamellar Structure and Chain Segregation in Lyotropic Liquid Crystals of Poly(5,7-Dodecadiyne-1,12-Diol Bis[[(4-Butoxycarbonyl)Methyl]Urethane]). *Macromolecules* **1994**, *27*, 1027–1032.

MA070998J